Marine and Environment Volume 12 Issue 1 (2023)
doi: 10.18686/me.v12i1.9490

Original Research Article

Seismic stratigraphy and structural analysis in the determination of petroleum play within Salin basin, Myanmar

Sai Naing Lin Aung[1,*], Win Maw[1], Aung Moe[2], Kyi Nwe Nwe Aung[3], May Thu Thu Aung[4]

[1] *Department of Geology, University of Yangon, Ministry of Education, Yangon 11041, Myanmar*

[2] *Independent Researcher, Saarlandstr 40, Ludwigshafen 67061, Germany*

[3] *Department of Geology, Dagon University, Ministry of Education, Dagon 11422, Myanmar*

[4] *Department of Geology, Panglong University, Ministry of Education, Pinlon 06114, Myanmar*

*** Corresponding author:** Sai Naing Lin Aung, snla.sainainglinaung@gmail.com

ABSTRACT

This study presents a new interpretation of the seismic stratigraphic unit equivalent to the Late Cretaceous to Pliocene formations in the Salin basin. Many researchers investigated the outcrops of the stratigraphic succession of the Salin basin but there is a lack of comprehensive analysis by seismic interpretation. This study provides a comprehensive description of the structural development within the Salin basin, enhancing our comprehension of the regional stratigraphic evolution of the examined region. Seismic sequences were delineated using a combination of horizon mapping, internal reflection configuration, termination patterns, and thickness analysis. We identified two distinct mechanisms for lateral fault seals: (1) primary juxtaposition seals and (2) secondary fault rock seals (also known as membrane seals). Once the hydrocarbons are matured within the source formations (Late Cretaceous to Early Oligocene shales units): Kabaw (KB); Laungshe (LA); Tabyin (TA); Pondaung (PO); Yaw (YA); and Shwezettaw (SZT), they are migrated towards the reservoir formations (Pondaung (PO), Shwezettaw (SZT), Padaung (PA), Okhmintaung (OHK), and Kyaukkok (KK)) through these predicted paths. Generally, the primary migration takes place along the fault or fractured planes or pores within rock units. In the southwestern limb of the Yenangyaung anticline, the disharmonic folding and upward bending of the KK, PY, OHK, and PA formations resulted in the deformation of ductile strata within the PA Formation, forcing them towards the peripheral synclines. The main deep fore-thrust in the southwestern limb of the Chauk anticline rooted within the PA Formation flattened up while approaching the OHK and PY formations. Chauk anticlinal axis above the PY and OHK detachment level are more migrated toward the northeast. As a result, above the crest of the deep anticline, the shallow low-angle fore-thrust pushed up into the growth strata, leading to the uplift of the YA and SZT formations within the Letpando anticline. YA Formation crops out locally along the axis of the structure and is the major seal, with sandstones in the underlying Eocene PO Formation being the main reservoir.

Keywords: seismic stratigraphy; petroleum play; Salin basin; structural analysis

ARTICLE INFO

Received: 4 August 2023
Accepted: 7 September 2023
Available online: 7 December 2023

1. Introduction

The Salin basin is one of the sub-basins in the greater Central Basin (CB) which is located from latitude 19°05′ N to 22°0′ N, with a width and longitude of 94°55′ E to 95°50′ E (**Figure 1**). The Salin basin covers an area of roughly 20,000 square km (200 × 100 km) and comprises deposits of up to 15 km of Tertiary shale, siltstone, sandstone, and coal. This basin is one of the most important petroliferous onshore sub-basins in Myanmar. This basin comprises both transgressive marine and regressive fluvio-deltaic conditions with a general north-south slope during the Eocene and early part of the Oligocene time[1,2]. The typical stratigraphic succession of the Salin basin is shown in **Figure 2**. The primary sources of Tertiary oils in this area are clastic rocks from the Eocene sediments (including the LA, TA, PO, and YA formations) and Oligocene deposits (comprising the SZT and PA formations). These rocks are abundant in organic-rich mudstone, carbonaceous shale, and oil shale, as highlighted by Htut[3] in 2017 and Aung et al.[2] in 2021. The primary oil reservoirs consist of formations from the Middle and Late Eocene (specifically the TL and PO formations), the Oligocene (encompassing SZT, PA, and OHK formations), and the Early-Middle Miocene sandstones (PY and KK formations), as detailed by Htut[3] and Aung et al.[2] in 2021.

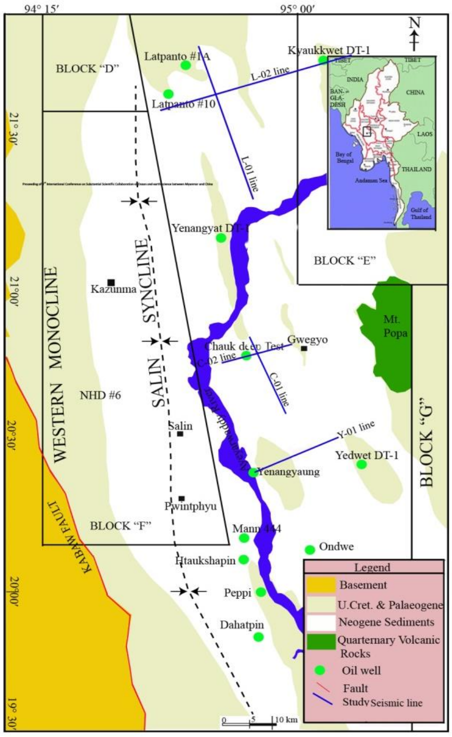

Figure 1. Outline map of the Salin basin, showing the locations of oil fields and study seismic lines.

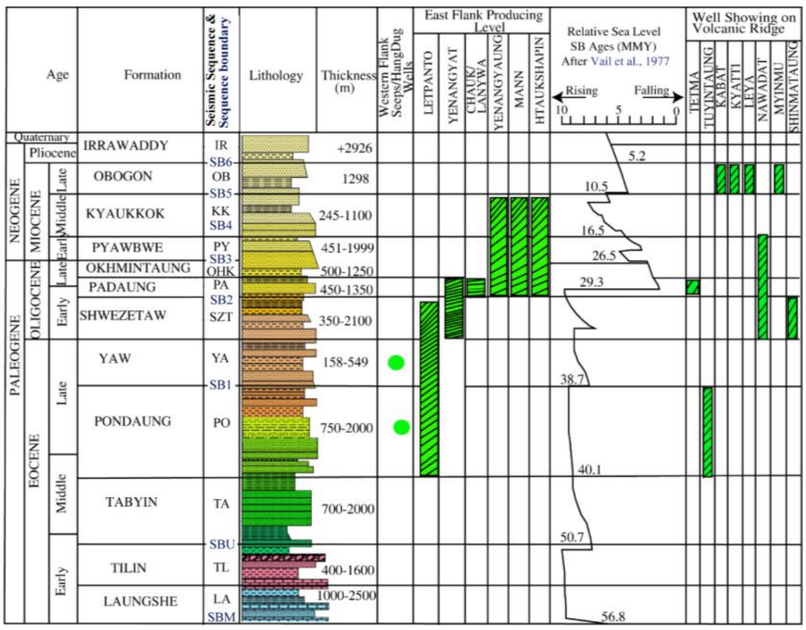

Figure 2. Generalized the petroleum reservoir formations and sequence stratigraphy of the typical section of Salin Sub-basin. The section is a composite of the Paleo column after Vail et al.[17].

Note: Variuos sequence boundaries associated with MFS maximum flooding surface, HST high stand tract and TST transgressive system tract except lower Padaung SB2 sequence boundary consisting of IVF incised valley fans Palaeocene Paunggyi 1888 m. Cretaceous Kabaw 1300 m and Triassic Thanbava 2750 m are not shown in this figure.

Seismic sequences were established through a combination of horizon mapping, the analysis of internal reflection patterns, termination patterns, and thicknesses. These features were identified in five seismic lines and demonstrate the continuity of the Late Cretaceous to Pliocene formations throughout the Salin basin. In the study area, all seismic sequence boundaries are demarcated using continuous markers with strong amplitudes, ranging from fair to good quality. Faults and their movement histories are important elements of the hydrocarbon migration and entrapment system within sedimentary basins[4–9]. Their predictions regarding the sealing properties of faults were grounded in the analysis of factors such as the geometry and lithological attributes of the faulted sequence, the configuration of the fault surface, and deformation parameters[10–14]. The identification of gas chimneys provides a clue for the existence of hydrocarbons and assists in understanding the petroleum system of a region.

2. Tectonic setting and regional geology

The Salin basin is bounded by Indo-Myanmar (Burman) Ranges (IMR) in the west, Chindwin Basin in the north, Shan Plateau in the east, and Pyay Embayment in the south. During the earliest Oligocene period, the IMR was uplift, leading to its separation from the eastern portion of the Central Basin (CB) and the western part of the Rakhine coastal belt[15]. Tectonically, this basin is interpreted as a complex forearc/backarc basin and it extends about 195 km in a north-south direction[16]. The orogenic movement associated with sedimentary fold-thrust structure implies the addition of recycled materials and created the continental crustal formation of IMR[16]. The Salin basin is separated by the Kabaw Fault complex into the basement rocks of the IMR which are reported by Pivnik et al.[16]. At the end of the Oligocene, the area was slowly uplifted and probably a slight fold took place at the present major structural units of the Salin basin.

The Salin basin is divided to the east by the younger thrusted Ngashandaung-Gwegyo-Tuyintaung anticline and to the west by older thrust-related Suwin-Kyaukkwet-Sabe-Yenangyat-Chauk-Yenangyaung anticline[16]. These anticlines generally align parallel to the basin's overall NNW orientation. The Yenangyaung and Chauk anticlines serve as typical major oil traps in Myanmar.

The Salin basin encompasses sedimentary rock formations spanning from the Late Cretaceous to the Pliocene, with a predominant layer of Late Miocene to Pliocene sediments, notably the Irrawaddy Formation, which boasts a thickness ranging from 3000 to 4000 m (see **Figure 2**)[3,18,19]. The basin's sediments are primarily derived from the eastern part of the Indo-Myanmar Ranges (IMR), which experienced collision and uplift. These sediments were transported by various major river systems, including the Irrawaddy River, as the Indian Plate migrated from the east to the north[20]. The Pre-rift sediments of the Salin basin include limestone, shale, and sandstone of KB Formation (Late Cretaceous). Clastic sediments of Paleocene Paunggyi (PG) Formation and Eocene Sequences (LA, TL, TA, PO, and YA formations) are deposited as rift sediments and Oligocene-Miocene sequences of Pegu Group such as SZT, PA, OHK, PY, KK, OB formations represent the Syn-rift sediments[19,21]. Middle Miocene to Pliocene sediments of the Irrawaddy Formation were post-rift sediments.

3. Methodology

Six representative seismic profiles were interpreted for sedimentation and structures. Interpretation of the stratigraphic development of the Late Cretaceous to Pliocene Formation in the study area is based on one-dimensional seismic data, ranging from poor to good quality. A seismic type section in the southern part of the study area is defined on seismic lines Y-01, and Y-02, as well as the central part, is based on C-01, and C-02 seismic lines (**Figure 1**). The seismic interpretation for the northern part of the Salin basin is based on L-01 and L-02 seismic lines (**Figure 1**). These studied seismic line sections are showing anticlines and several associated faults, indicating stratigraphic geometry (**Figures 3–8**) and are used for seismic stratigraphic interpretation, oil and gas migration, accumulation, trap, and seal for the Salin basin. The seismic stratigraphy analyses are designated by the seismo-stratigraphic units identified in the seismic data such as the geometry of the reflectors, stacking patterns, continuity, and amplitude of seismic waves[22,23]. Wornardt[24] indicated that the seismic sequence stratigraphy analysis is used for the integration of high-resolution biostratigraphy, paleobathymetry, well-log signatures, and seismic-reflection profile. The presence of hydrocarbon seepage, both liquids, and gases in the Salin basin is a dynamic characteristic of hydrocarbon systems in Myanmar due mainly to the vertical and/or lateral hydrocarbon migration.

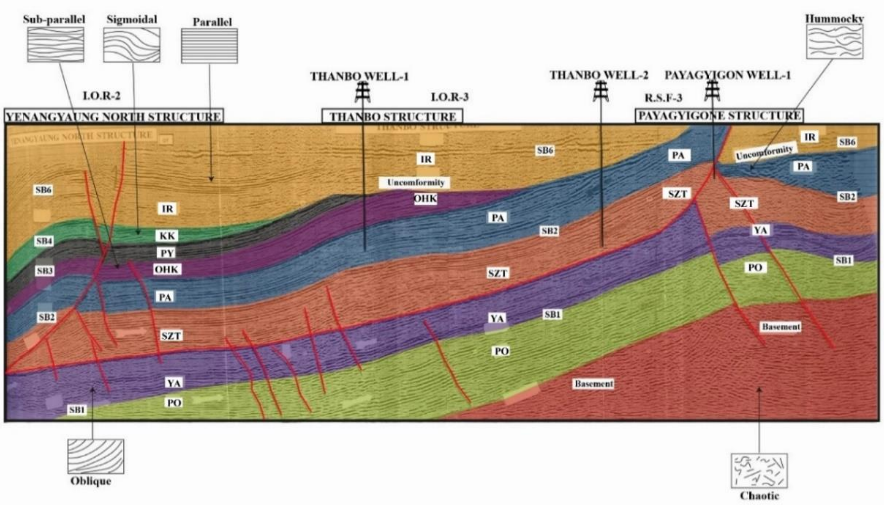

Figure 3. Seismic reflection patterns visually identified from seismic data (Y-02 line).

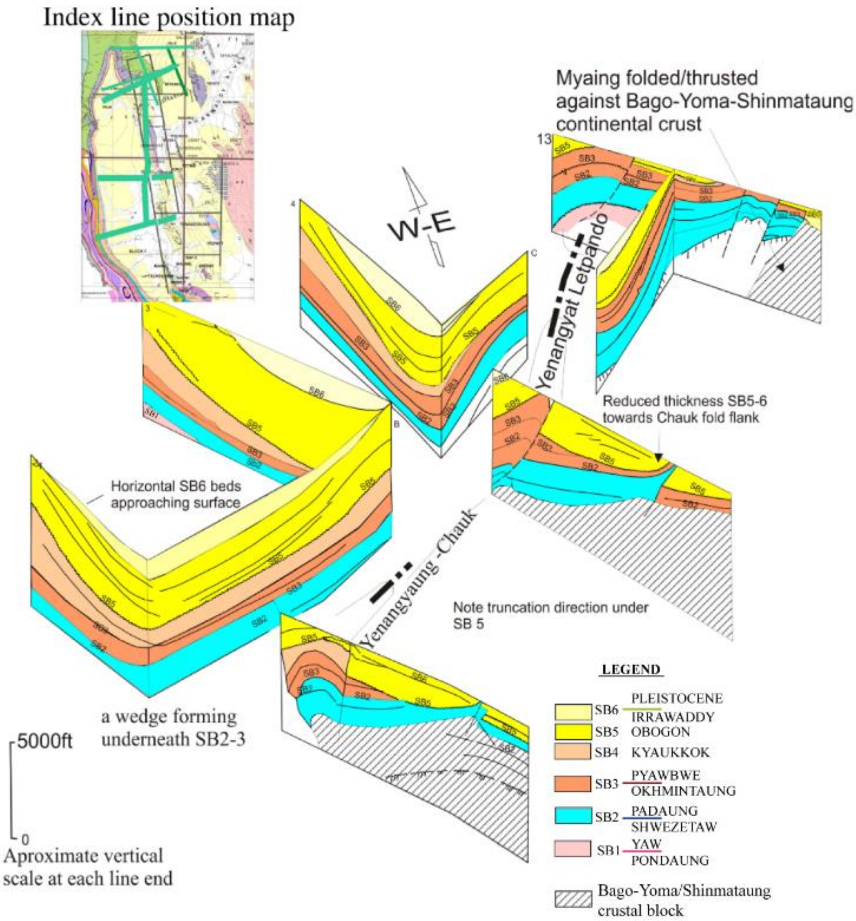

Figure 4. Fence diagram of transverse and longitudinal seismic profiles with tectonic and stratigraphic interpretation in the Salin Sub-basin showing the stratigraphy pattern of the basin.

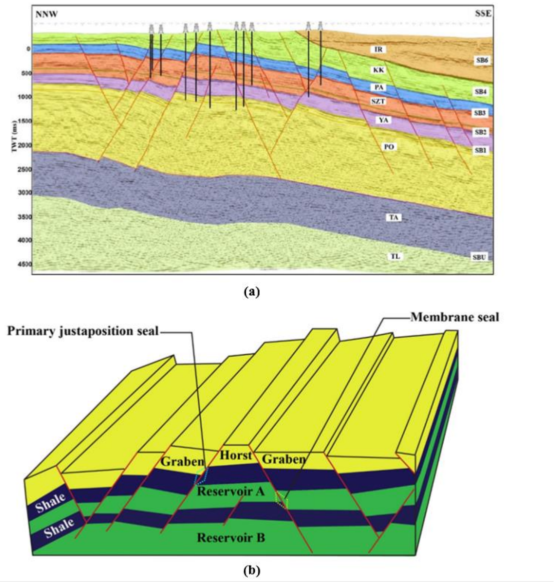

Figure 5. (a) Two-way travel time (L-01 line) NNW-SSE seismic section across Letpando oil field; **(b)** Schematic illustration displays potential hydrocarbon traps subsequent to normal faults that offset a sand-shale sequence.

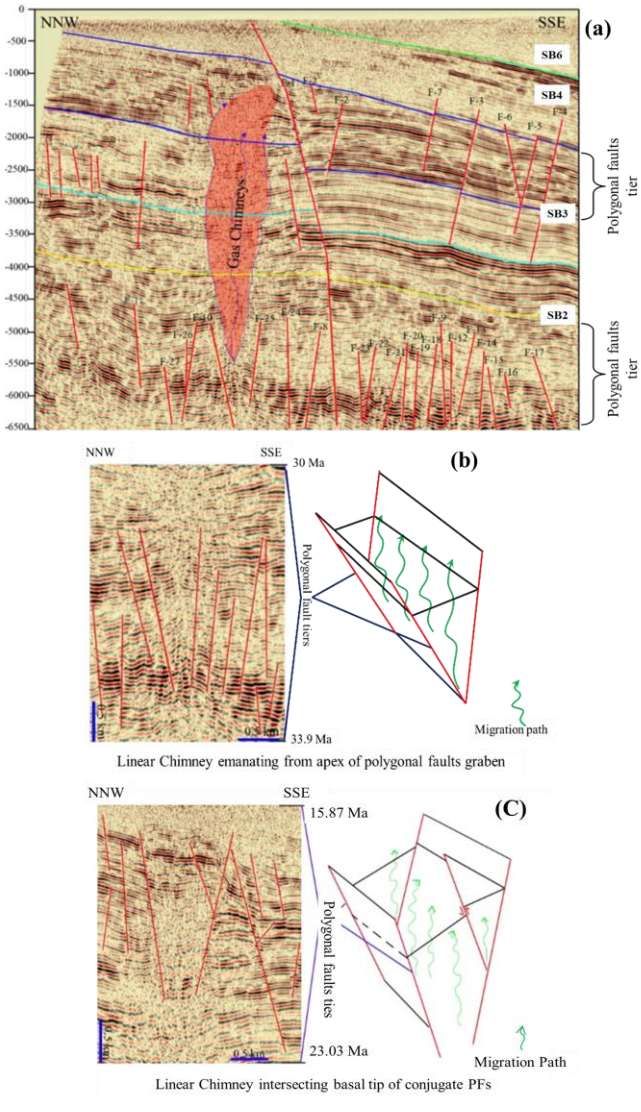

Figure 6. Linear Chimneys intersecting and emanating from different parts of the polygonal faults (PF) planes in seismic line (C-01 line) **(a)** The linear plan from the geometry of the chimney is shown on a series of amplitude maps, the chimney intersects the apex of the underlying PF graben **(b)** and **(c)** Seismic section showing chimney intersecting the basal portion of conjugate polygonal faults.

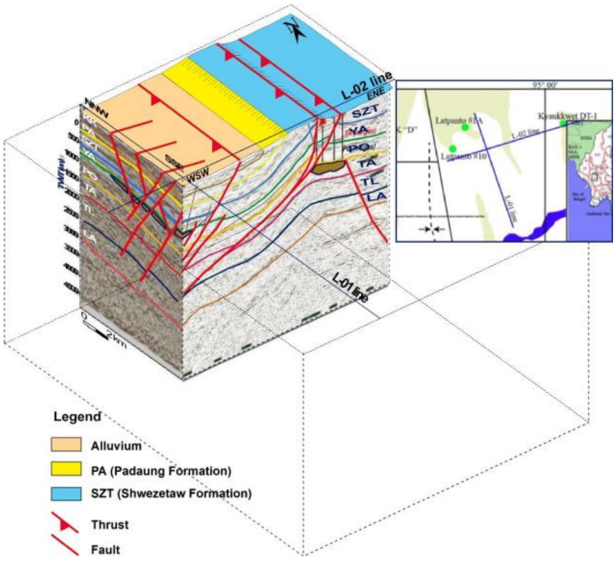

Figure 7. 3D diagram construction from seismic profile (two ways travel line L-01 line and L-02 line) of Letpando oil field, showing the hydrocarbon trap in the PO (Pondaung Formation) and TA (Tabyin Formation) at the anticlinal crest of Lepando and Kyaukkwet.

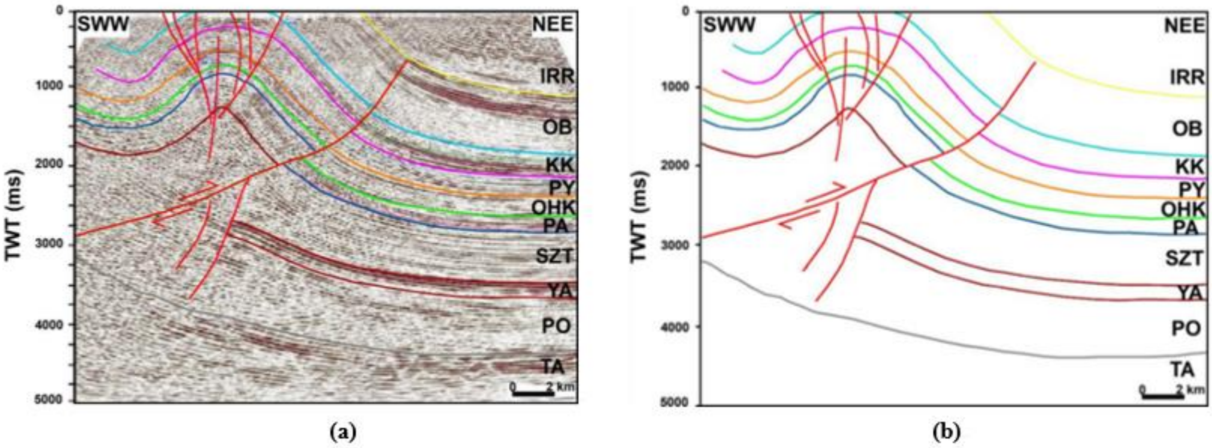

Figure 8. (a) Geological interpretation of two-way-travel time millisecond—TWT (ms)—time-migrated seismic profile Y-01 line through the northwest part of the Yenangyaung anticline; **(b)** Geological interpretative cross-section of seismic profile Y-01 line.

4. Oil field belt in Salin basin

The Salin basin currently hosts several oil fields in commercial production, including Letpando, Yenangyat (with major domes such as Payani, Yenangyat, Pauktaw, Sabe, and Thagyitaung in the north of Sabe), Chauk, Yenangyaung, Mann, Htaukshabin, and Kanni (**Figure 1**). These fields primarily exploit Oligocene and Miocene sands found within the Padaung, Pyawbwe, and Kyaukkok formations. By examining selected seismic profiles and considering the tectonic evolution inferred from geological data, correlations have been established between the stratigraphic sequence boundaries (SB) and the current reservoir beds in each field. A comprehensive analysis, combining biostratigraphic and lithological sequences, has been conducted in all potential fields, which include Kyaukkok, Pyawbwe, Okhmintaung, Padaung, Shwezettaw, Yaw, and Pondaung (see **Table 1**). In the Yenangyat-Chauk, Yenangyaung, and Minbu anticlines, the primary oil producers are the Oligocene-Miocene Beds. Notably, the Early Oligocene Shwezettaw Formation, despite its predominantly continental nature across the region, serves as a suitable reservoir rock. Additionally, the Middle Oligocene Padaung Formation, while predominantly argillaceous, contains increasing percentages of arenaceous material toward the east, making it a significant source and reservoir rock[25]. **Table 1** provides an overview of the production reserves for the oil field belt within the Salin basin. The nature of the structure and the abundance of fault make the occurrence of large accumulations of hydrocarbons unlikely except perhaps at relatively great depths. Hence, any oil or gas findings at shallow depths within structural or stratigraphic traps are unlikely to be substantial. This is supported by the presence of source rocks in both the Eocene and Miocene periods, characterized by argillaceous formations like the Tabyin, Yaw, and Pyawbwe, which were deposited under marine conditions. The Eocene sequence has limited suitable reservoir rocks, primarily consisting of fine-grained and argillaceous formations, except for the lower section of the Pondaung Formation. In contrast, Miocene arenaceous rocks generally exhibit more favorable reservoir properties.

In general, the basin of deposition becomes deeper towards the east and south of the Thayetmyo area and therefore the sandstone in these parts is usually finer-grained and more argillaceous. Thus, the structures on the north-western margin of the area are better placed than those in the south and east.

Table 1. The production history of oil fields in Salin basin.

Oil fields	**Discovery (year)**	**Sands**	**Total net pay sand (ft)**	**OIIP (MMBL)**		**GIIP (Bcf)**		**Recovery (%)**	**Formation wise hydrocarbon distribution of the fields**					
				Reserve	Commutative production	Reserve	Commutative production		Kyaukkok	Pyawbwe	Okhmintaun g	Padaung	Shwezetaw	Pondaun g
Letpando	1974	-	-	76.8	2	-	-	0.4	-	-	-	-	0.28	1.42
Kyaukkwet	1995	-	-	41	0.28	-	-	-	-	-	-	-		
Thargyitaung	2001	-	-	130	1.1	-	-	-	-	-	-	1.1	-	-
Sabe + Yenangyat	Pre War	-	-	32	8	-	16 Bcf (1963–1983)	-	-	-	-	-	1.21	-
Chauk + Lanywa	1901	10	410	400	154	-	-	37	-	-	-	147.37	-	-
Yenangyaung	1887	28	901	561	200	115	39	41	29.97	74.12	89.14	30.76	-	-
Mann	1970	25	535	689	111	-	-	25	13.99	32.72	39.34	20.28	-	-
Htaukshapin + Yethaya	1978	27	1250	713	21	-	-	13	17.88	0.82	1.14	0.13	-	-
Kanni + Peppi	1985	12	550	56	12	-	Kanni 49, Peppi 88	-	6.09	0.01	-	-	-	-
MMBL-Million Barrels, Bcf-Billion Cubic Feet, OIIP-Oil Initially in Place, GIIP-Gas Initially in Place							Total MMBL		63.93	107.67	129.62	200.17	1.49	1.42

5. Interpretation of seismic stratigraphy

A geological entity's structural and stratigraphical interpretation is important for expediting hydrocarbon exploration[26]. The detection of subsurface geology and identifying potential hydrocarbon prospects in the study area, seismic data, complemented by well information, is analyzed on an interactive workstation. This analysis involves measuring the two-way travel time (TWT) of seismic waves within the seismic section as they traverse geological layers, reflecting off surfaces after passing through the interfaces between these contracting geological strata[27].

Figures 3–10 show the seismic facies analysis, including the delineation of internal reflection geometry, continuity, frequency, and internal velocity. Internal reflections provide insights into the deposition history of a particular unit, while external reflection terminations, such as onlap and downlap, can serve as indicators of facies boundaries and limitations. Seven sequence boundaries and fourteen seismic sequences were identified within the study area. In ascending order, the seismic sequences are KB, PG, LS, TL, TA, PO, YA, SZT, PA, OHK, PY, KK, OB, and IRR, as well as the seismic sequence boundaries, are SBM, SBU, SB1, SB2, SB3, SB3, SB4, and SB6 (**Figures 3–10**).

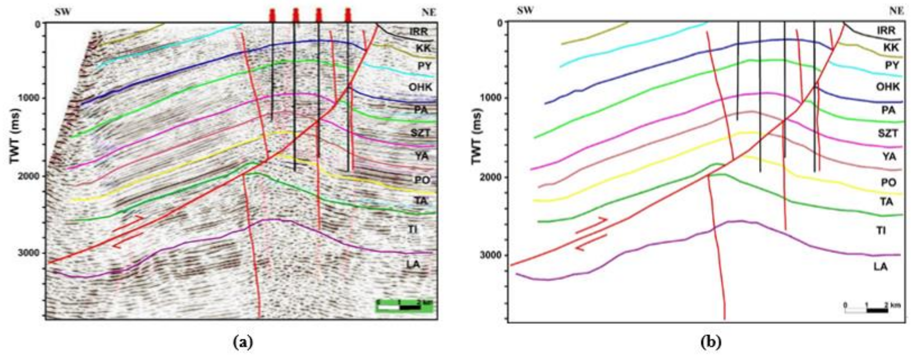

Figure 9. (a) Time-migrated seismic profile (C-02 line) through the northeastern flank of the Chauk anticline; **(b)** Geological interpretation of this profile indicates a main deep fore-thrust in the northeastern limb rooted within the PA Formation.

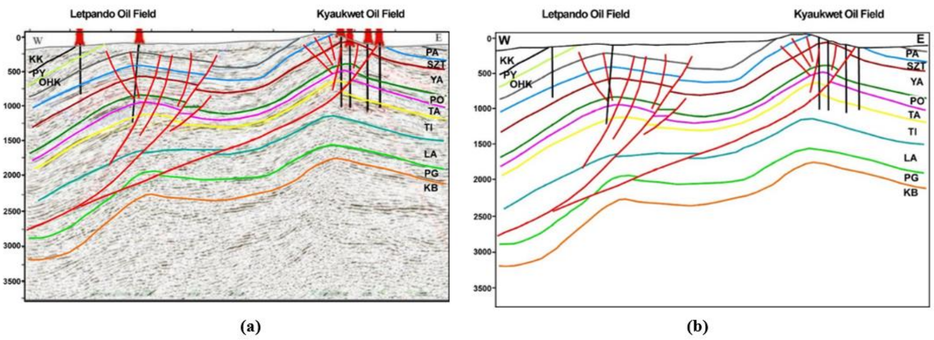

Figure 10. (a) Time-migrated seismic profile (L-02 line) along the Letpando and Kyaukkwet anticlines; **(b)** Geological interpretation of this profile showing the main deep-thrust through the eastern limb of Salin Sub-basin as an evolution of detachment folding to fault-related fold as break-thrust fold.

The effect of the uplifting at 22° N high during the Middle-Late Oligocene, SB3 sequence was not observed in seismic sections (L-01 and L-02) from the northern part of the Salin basin (**Figure 4**). During the Middle to Late Miocene, the sea level was 220 m above the present sea level, at which time Bago Yoma volcanic line was uplifted and attained a large landmass. The Middle and Late Miocene regression is seen in all SE Asian basins as unconformities and a general regressive cycle containing sub-cycles. The unconformity that occurs between the SB6 and SB4 facies probably does not represent a significant amount of erosion (**Figure 4**). **Figure 4** shows the fence diagram of transverse and longitudinal seismic profiles with tectonic and stratigraphic interpretation in the Salin Sub-basin.

5.1. IRR sequence (late Miocene-Pliocene)

The first and topmost section is the IRR sequence, its underlying units by a Late Miocene unconformity (**Figures 3–9**). It can be identified on the seismic sections by the presence of low-amplitude internal reflections. Two-way travel time through seismic sequence IRR ranges from about 0 to approximately 500 milliseconds and its thickness ranges from about 3000 to 3500 m. The seismic sequence IRR is underlain by the seismic sequence KK. The average energy attribute proves highly valuable for delineating the upper boundaries of seismic sequences as it typically forms a traceable, continuous high-energy event (black end of high-energy attribute color range) that is highly reflective. The shale unit is present at the lowermost surfaces of the seismic sequence IRR. The parallel to the subparallel configuration of reflections within the IRR sequence indicates a spatially uniform sedimentation rate[28,29] (**Figure 3**). IRR Formation is mainly comprised of fluvial sandstone and shale, which are widely distributed within this basin.

5.2. OB sequence (middle Miocene)

The Middle Miocene Obogon Formation contains light grey, soft to moderately hard, thinly bedded, fine to medium-grained sandstone interbedded with olive-grey to dark grey, soft, laminated, micaceous and carbonaceous thinly laminated shales. Gritty sandstones are occasionally intercalated with bluish and light grey shale. This sequence is only observed in the northeastern part of seismic line Y-01 (Yenangyaung Oil field) (**Figure 8**). The seismic reflection pattern is characterized by high-amplitude internal reflection in the upper part and low internal reflection in this sequence (**Figure 8**). According to Aung[18], the Obogon Formation was deposited during storm episodes and within a transgressive estuarine environment, as determined through a lithofacies analysis.

5.3. KK sequence (early Miocene)

The KK sequence is bounded by IRR at its top and PY at its bottom. Strata within this unit show sub-parallel and it's characterized by low to moderate internal reflections (**Figures 3–9**). Two-way travel time through the seismic sequence KK ranges from about 500 to approximately 700 milliseconds and its thickness ranges from about 760 to 900 m. The top sequence of IRR coincides with a regional unconformity of the Late Miocene age. The uppermost seismic reflections of the seismic sequence KK are terminated against faults (**Figures 6** and **9**). Locally, the seismic reflections display erosional truncation along the top of the seismic sequence KK (**Figures 6** and **9**). Strata within this unit show sigmoidal and it's characterized by low to moderate internal reflections (**Figure 3**). The KK sequence mainly comprises the delta front and delta plain which is composed of sandstones interbedded with brown shale beds[30]. According to Beard and Weyl[31], the physical and mechanical characteristics of the KK sandstone have an excellent reservoir quality to store oil and gas.

5.4. PY sequence (early Miocene)

This seismic sequence PY is superjacent to the seismic sequence KK and subjacent to the seismic sequence OHK (**Figures 3**, **6** and **9**). Typically, the seismic reflections of seismic sequence PY are comparatively distinct from seismic reflections above and below in that they have a noticeably higher amplitude (**Figures 3**, **6** and **9**) and average energy. Strata within this unit show sub-parallel and it's characterized by high internal reflections (**Figures 3**, **6** and **9**). Two-way travel time through seismic sequence PY ranges from about 700 to approximately 1000 milliseconds and its thickness ranges from about 600 to 800 m. The PY sequence comprises shallow marine shale with a high content of mica, slight carbonaceous material, and gypsum[32,33].

5.5. OHK sequence (late Oligocene)

This seismic sequence OHK is superjacent to the seismic sequence PA and the seismic sequence PY (**Figures 3**, **6** and **9**). The seismic sequence OHK is mainly composed of deltaic to shallow marine sandstones and shales[34]. In the central region of the study area, the two-way travel time within the seismic sequence OHK spans approximately 700 to 1000 milliseconds, with a thickness ranging from approximately 1200 to 1300 m. Typically, the uppermost and lowermost sections of the seismic reflections of OHK are comparatively distinct from the PA and PY sequences in that they have a noticeably higher amplitude than the OHK sequence. Strata within this sequence show subparallel (**Figures 3**, **6** and **9**). Additionally, a substantial number of crestal faults have been identified within this formation (as shown in **Figures 6** and **9**).

5.6. PA sequence (middle Oligocene)

The PA sequence is bounded by the OHK sequence at its top and the SZT sequence at its bottom (**Figures 3, 6–10**). Within the seismic sequence PA, the two-way travel time spans approximately 2700 to 3700 milliseconds, and its thickness varies from about 600 to 800 m. This sequence primarily consists of marine shales interlayered with sandstones. The hummocky reflection pattern is characterized by high-amplitude internal reflection and continuous reflections in this sequence (**Figure 3**). According to the reservoir characteristics of the PA sandstone, it is a good store reservoir for oil and gas[35] and the Chauk oil field is currently producing oil and gas from the PA Formation.

5.7. SZT sequence (early Oligocene)

The SZT Formation is underlain by the PA sequence (**Figures 3**, **5**, **6**, **9**, and **10**). Two-way travel time through the seismic sequence SZT ranges from about 1100 to 1400 milliseconds and its thickness ranges from about 750 to 800 m. This sequence is mainly comprised of shallow marine to alluvial sandstone and shale, locally presenting the thin coal seam[36]. The SZT sequence is widely distributed in the northern part of the study area (around the Latpando and Kyaukkwet oil fields). Strata within this sequence show sub-parallel, high-amplitude internal reflections with good lateral continuity. The uppermost part of this sequence is characterized by chaotic internal reflections and by the presence of faulted intervals (**Figures 6** and **9**). In the northern part of the study area, reflection configurations are parallel and sub-parallel to the upper boundary of the seismic sequence PA (**Figures 3**, **5** and **10**), as well as in the central and southern parts of the study area, seismic reflections downlap onto the lower boundary of the seismic sequences (**Figures 5** and **7**).

5.8. YA sequence (late Eocene, Priabonian)

In **Figures 3**, **5** and **10**, the YA Formation is underlaid by the SZT Formation and overlaid by the PO Formation. Two-way travel time through seismic formation YA is approximately 1500 to 2000 milliseconds in the northern part of the Salin basin. **Figures 3** and **7** show seismic lines from the Letpando and Kyaukkwet oil fields, where the thickness ranges of the YA Formation are from approximately 300 m to 450 m. This formation is mainly comprised of estuarine sediments of shale and clay, local gypsums, and occasional scattered wood fossil fragments in the clays[37]. In the seismic line (**Figure 3**), the YA Formation shows oblique reflections and a high-amplitude international reflection. Aung et al.[2] suggested the YA Formation is a potential source of rock for oil and gas based on the geochemical results.

5.9. PO sequence (late Eocene, Bartonian)

The seismic sequence of PO is superjacent to the seismic sequence YA and subjacent to the seismic sequence TA (**Figures 3**, **5** and **10**). The seismic sequence of PO is mainly composed of terrestrial mudstone, sandstone, and conglomerate[38–40]. Two-way travel time through the seismic sequence PO is approximately 1500 to 2800 milliseconds in the northern part of the study area, especially the Letpando and Kyaukkwet oil fields. The ranging thicknesses of PO are from approximately 1050 to 1200 m. PO sequence was deposited in swampy brackish water and nearshore fluvial environments. In the Kuakkwet oil field, oils are produced from PO Formation, but reservoir characteristics of the PO Formation are not quite favorable (low porosity and permeability).

5.10. TA sequence (middle Eocene, Bartonian)

The TA Formation is bounded by PO at its top and TL at its bottom. Strata within this unit show sub-parallel and it's characterized by moderate internal reflections (**Figures 5** and **10**). Two-way travel time through seismic sequence TA ranges from about 2800 to approximately 4000 milliseconds and its thickness ranges from about 900 to 1050 m. The TA Formation is mainly composed of marine fissile shale interbedded with buff color medium-grained argillaceous sandstone[41]. Aung et al.[2] suggested that the TA sequence is comprised of mudstone with shallow marine shale which matures and over matures for oil generation based on the organic geochemical results.

5.11. TL sequence (middle Eocene, Lutetian)

In **Figures 5** and **10**, the lowermost sequence is the TL Formation and is overlain by the TA Formation. The TL sequence is mainly comprised of outer shore sandstones interbedded with abyssal carbonaceous shale. Two-way travel time through seismic formation TL ranges from about 4000 to above 4500 milliseconds and its thickness ranges from about 900 to 1200 m. Strata within this sequence show sub-parallel, low to moderately-amplitude internal reflections with fair lateral continuity. TL sequence was deposited under the outer shoreface to abyssal conditions.

5.12. LA sequence (early Eocene)

In **Figures 9** and **10**, the early Eocene LA sequence is underlain by the TL sequence. The TL sequence contains mainly shales, interbedded with a few sandstone and fossiliferous limestone beds (packstone and wackestone). Dark-grey colored laminated to nodular, carbonaceous shales are interbedded with light grey to buff color argillaceous sandstone of LA sequence. Two-way travel time through seismic formation LA ranges from about 2500 to above 2800 milliseconds and its thickness ranges from about 1000 to 1800 m. Strata within this sequence show sub-parallel, low to moderately-amplitude internal reflections with fair lateral continuity. Lwin et al.[41] revealed shales interbedded with fossiliferous limestone occupied the northern part of the Salin basin. The LA sequence was deposited on a shelf in deep-marine environments.

6. Fault-sealing behaviors

The northern part of the Salin basin, specifically the Letpando and Kyaukkwet oil fields area, presents a structurally complex area. Evaluating lateral fault seals in this part of the study area involves considering several critical factors. Here, we concentrate on the problem of cross-fault flow between the stratigraphic units on either side of the fault surface. Movements along fault surfaces result in the displacement of stratigraphic units within the hanging wall relative to those in the footwall. This displacement can either facilitate or hinder the flow of hydrocarbons across faults, thereby influencing hydrocarbon entrapment, particularly when the fault juxtaposes impermeable units against potentially reservoir-bearing units (**Figure 5**).

In seismic section L-01, two distinct mechanisms for lateral fault seals are observed: (1) primary juxtaposition seals and (2) secondary fault rock seals, commonly referred to as membrane seals (**Figure 5(b)**). This nomenclature generally follows that used in recent studies[42–44]:

(1) **Primary juxtaposition seals**: In this type of seal, a fault displaces a sealing lithology, typically the upper seal, into juxtaposition against the reservoir. The key evidence supporting this sealing mechanism is the impermeability of the juxtaposed material over a geological time period. We simply refer to this sealing mechanism as a "primary seal" or "primary juxtaposition seal". The primary juxtaposition seal is established when an impermeable lithological layer (e.g., shale) comes into contact with a reservoir lithological layer at the fault location[45]. In the seismic section (as seen in **Figure 5(b)**), the lithologies of reservoir A (SZT Formation) and B (PO Formation) from one fault block are juxtaposed against non-reservoir shale lithologies (PA and YA Formations) from the opposing fault block. This juxtaposition can involve different sediment units

such as sand/sand, sand/shale, or shale/shale, depending on the juxtaposed materials along the faults. For example, reservoir sands may be juxtaposed against a low-permeability unit (e.g., shale) with a high capillary entry pressure[46].

(2) **Secondary fault rock seal (membrane seal):** This type of seal is also known as a membrane seal or capillary seal. It is based on the concept that fault-zone material (referred to as fault rock) acts as a lateral seal due to fault-induced reductions in grain size, the transport of fine-grained material along the fault zone, and/or subsequent chemical processes that create a continuous, low-permeability zone with a high capillary entry pressure. We designate this sealing mechanism as a “secondary seal”. Various processes have been proposed to explain the generation of membrane seals, considering factors such as fault rock capillary access pressure and permeability. In this context, a seal is formed along the fault plane when a lithology with a pore radius is reduced to a point where it falls below the permeability threshold at a specific pressure regime (such as a high shale content, which can be assessed through the shale gauge ratio SGR).

7. Gas chimneys

Gas chimneys represent a type of disorderly vertical disturbance observed in seismic data, characterized by discontinuous reflectors and weaker reflection amplitudes[47]. Recognizing gas chimneys serves as a valuable indicator of potential hydrocarbon presence and contributes to a deeper understanding of the petroleum system within a region. This also identifies potential over-pressured zones in mitigating the drilling risks[48]. Chimneys, as interpreted from seismic data, manifest as narrow, vertical zones with stacked amplitude anomalies[49–51], which may coincide with seismic pull-up or push-down (**Figure 6**). Chimneys can signify various geological phenomena, including mud diapirism, active gas seepage, potential migration pathways, or the presence of hydrocarbon reservoirs themselves[52].

The seismic sections, as illustrated in **Figure 6**, reveal that linear chimneys intersect or terminate at various positions along individual polygonal fault planes, spanning from the base to the uppermost tip, with some intersections being either absent or indeterminate. These linear chimneys originated during the Oligocene to Early Miocene period, approximately 33.9 to 15.97 million years ago. They primarily exhibit a vertical orientation and are predominantly formed within an interval affected by widespread, closely spaced normal faulting. These layer-bound faults, as depicted in **Figure 6**, delineate a somewhat “polygonal” pattern when viewed on a map. Linear varieties of fluid flow are evident as shallow depressions resembling small pockmark-like structures. The chimneys intersect the apex of the underlying graben formed by polygonal faults, as shown in **Figure 6(a)**. In **Figure 6(b)**, the chimney intersects the basal section of conjugate polygonal faults.

A subset of chimney stems and polygonal faults offers valuable clues for establishing the timing of each fluid flow structure. The growth of polygonal faults is believed to have taken place during either the deposition or burial of stratigraphic layers[53]. Typically, polygonal faults are associated with specific seismic horizons within a narrow timeframe spanning from the Early Oligocene to the Early Miocene. We also consider that this Early Miocene polygonal faulting, which occurred at the beginning of the Pliocene, before the phase of fluid flow that formed overlying linear shallow depressions and chimneys.

The linear Chimneys provide a clear indicator of the migration pathway that gas took on its ascendancy through the polygonal faulted stratigraphy. If the polygonal faults had served as the primary migration pathway, we would anticipate that linear chimneys would consistently terminate downward at the uppermost tips, or at least the uppermost footwalls, of these polygonal faults. The gas, therefore, originated from deeper sources and accumulated at over-pressured conditions beneath the tier of polygonal faults. Subsequently, the linear chimneys propagated vertically, intersecting and cutting across the planes of the polygonal faults (**Figure 6**). It is likely that gas may have migrated either obliquely along the lower sections of polygonal faults within the SZT Formation before reaching permeable layers within the PY Formation that abut the fault. Alternatively, the gas may have migrated more pervasively, moving through grain-to-grain permeability pathways.

8. Attribute analysis of seismic structures

Advanced techniques for attribute analysis were applied to the seismic profiles acquired around the Salin basin (**Figures 3–10**) to better evaluate fault and fracture probabilities within the vertical extent of seismic-sag structures and the associated potential for vertical cross-formational fluid-migration pathways. In addition, the fault-attribute zones extend upward from the lowermost limit of resolvable seismic-reflection data and within the SZT and PA Formations (**Figure 6**). A zone of coherent reflections is vertically sandwiched by zones that have a high probability of faults and fractures. In the seismic section (**Figure 6**), the first-order fault system extends through the entire stratigraphic column, resulting in significant vertical displacements of the strata. The second-order fault system exhibits a smaller vertical extent and induces less vertical displacement compared to the first-order faults. Additionally, various structural and stratigraphic characteristics are frequently observed in the Salin basin. These features are identified to assess the imaging capabilities of seismic data.

9. Migration pathways

Figure 5 shows an interpreted seismic line oriented along the NNW-SSE direction for the Letpando oil field. The fault analysis was carried out on dip lines as it provides a clearer picture of the fault pattern. Faults are marked in red color to differentiate between the horizon and vertical faults as it marked a discontinuity in the seismic reflectors. Tankard et al.[54] suggested that the Salin basin originated as a set of pull-apart basins during the early Eocene due to the northward movement of the Burma Plate relative to the Asian Plate, our seismic interpretation results indicate that the region predominantly exhibits normal faulting characteristics, albeit with some associated wrench components. The associated geometry is horst and graben in **Figure 5**; horst is the geologically uplifted part of the normal fault while graben is the downward portion of the fault which is bounded by two normal faults (**Figure 5**). The graben represents the deeper region where the likelihood of hydrocarbon accumulations is lower. In each formation, there is a distinctive horst and graben geometry. Hydrocarbons generally migrate from areas with higher potential or higher pressure to those with lower potential or lower pressure[26]. Consequently, the probability of hydrocarbon accumulation is primarily higher in horst structures rather than grabens. In the Letpando oil field, the predominant trap type is stratigraphic traps. The seismic section (**Figure 5**) reveals the presence of several normal faults.

Figures 3–10 illustrate lithologies that closely resemble actual subsurface conditions. The predicted pathways for hydrocarbon migration are indicated by green arrows. Once hydrocarbons reach maturity within the source formation, which consists of Eocene to Early Oligocene shale units, they migrate towards the reservoir formations (PO, SZT, PA, and OHK Formations) through these anticipated routes, as shown in **Figures 3–10**. Typically, primary migration occurs along fault lines, fractured planes, or through pores within rock units. The trace envelope rises in conjunction with the ultimate energy horizon on the seismic section, often correlating with substantial hydrocarbon accumulations that manifest as bright spots. The appearance of these bright spots is influenced more by the slope rather than the magnitude, indicating distinct interfaces.

10. Structural interpretation of seismic profiles

The seismic study was carried out in the Salin basin, particularly in the eastern part including Yenangyaung, Chauk, and Letpando-Kyaukkwet areas. The seismic lines are the Y-01 line of Yenangyaung anticline, the C-02 line of Chauk to Gwegyo anticlines, the L-02 line of Letpando to Kyaukkwet anticlines for the SW-NE direction, and the L-01 line of Letpando anticline for NNW-SSE direction. SW-NE direction seismic lines cross the regional strike and NNW-SSE direction seismic lines are along the strike of the area. The Salin basin is regionally known east vergence double plunging syncline[55].

The seismic profile Y-01 line is oriented NEE-SWW along the Yenangyaung anticline (**Figure 8**) in which deep thrust formed as east vergence through the fold, which breaks by thrust like a break-thrust fold (e.g., Fischer et al.[56] and Ghosh[57]). In the Yenangyaung anticlinal crest, the tension joints developed with the NNW-SSE direction, parallel to the fold axis, which is normal to the maximum compressive stress direction. The deep thrust in the seismic profile is the same as Yenangyaung Thrust. Miocene reservoirs trapping in the Yenangyaung Oil field by sinistral faults (**Figure 8**). Miocene valley exposure indicates the direction of divergent flows on both flanks of the Minlindaung EW traverse ridge, down to the Magwe NE region. In the Yenangyaung oil field, oils are explored from early and middle Miocene reservoirs rock.

The seismic profile L-01 line is oriented SSE-NNW along the Letpando anticline (**Figure 5**) parallel to the fold axis in which in the anticlinal crest, the cross faults developed with SWW-NEE direction, normal to the fold axis, which is parallel to the maximum compressive stress direction. However, these cross faults are activated as normal faults (gravity faults) to form the graben and horst structures by the shearing movement to develop the en-echelon faulting in the Central Myanmar Basin[58]. Lepando fold may be covered with Eocene sediment and the source for oil is flows expected to come from the Padaung or Yaw Formation below and entrapped within compartmentalized cross faults (**Figures 5** and **10**). Eocene reservoirs have been found in the northern part of the Letpando and Kyaukkwet oil fields.

Regarding Pivnik et al.[15], the Salin basin (**Figure 11**) is a syncline and in accordance with Khin et al.[55], the Salin basin is an east-vergence double-plunging syncline. Likewise, these seismic profiles indicate the progressive eastward compression to develop the detachment fold to fault-related fold due to the fault-propagation.

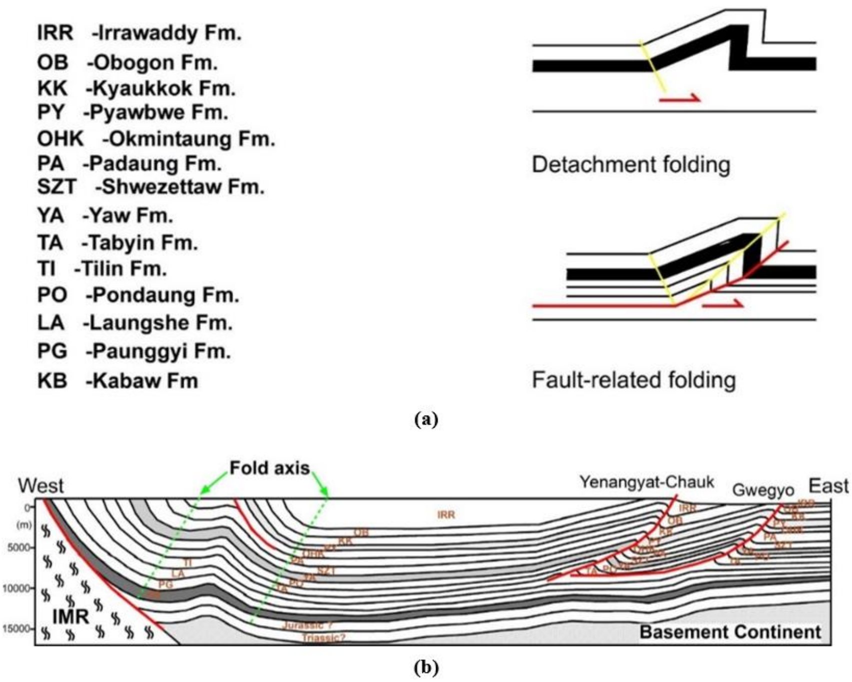

Figure 11. (a) Detachment folding and fault-related fold[56]; **(b)** Cross-section. through the Minbu-Salin Sub-basin showing the progressive compression to develop the detachment fold to fault-related fold at the Yenangyat-Chauk-Gwegyo area in the eastern part of Minbu-Salin Sub-basin (modified after Pivnik et al.[16]).

11. Folding geometry and interpretation of seismic profiles

We present an interpretation of the folding geometry within the Yenangyaung, Chauk, and Letpando-Kyaukkwet anticlines. Our analysis focuses on three selected seismic profiles situated in the eastern, central, and northwestern regions of these anticlines. The seismic lines orientation trend in a NE-SW direction. Within the seismic section spanning the Yenangyaung, Chauk, and Letpando-Kyaukkwet oil fields, we observe en-echelon arrangements of asymmetrical anticlinal structures. The axial planes of these en-echelon folds predominantly trend in a nearly N-S to NNW-SSE direction, (**Figure 11**).

One of the seismic profiles intersects the northeast termination of the Yenangyaung anticline, where the most significant brittle structure is characterized by ENE-directed major deep thrust faults, as shown in **Figure 8**. Above the tip of the deep thrust fault, strata exhibit considerable shortening primarily due to folding. In the intermediate areas, strata experience a combination of folding and faulting. The seismic section also reveals the presence of a Positive flower structure, primarily induced by transpressional deformation resulting from regional N-S dextral shearing. Additionally, ductile folding or transpression-related uplift is observed in the form of anticlines, flanked by steep-angle reverse faults striking northward, ultimately forming pop-up ridges.

The geometry of the fold axis below and above the PY and OKH formations are different. The fold axis above the PY and OKH detachment level are more migrated toward the northeast (**Figure 11**). The thickness of the IR Formation growth strata is increased due to the propagation of a deep-seated thrust. It could be deduced that the main deep-seated fore-thrust in the northeastern limb of the Yenangyaung anticline cuts up-section and flattens in the PY detachment. Disharmonic folding and upward bending of the KK, PY, OK, and PA formations squeezed the strata of the PA Formation in a ductile manner toward the peripheral synclines in the southwestern limb (**Figure 8**). The seismic profile depicted in **Figure 8** is situated in the central region of the Salin basin. This seismic line traverses the Chauk anticline, which exhibits strong asymmetry and trends in an NNW-SSE direction. The seismic line, denoted as seismic profile Y-01 line, runs along the NW-SE direction. On the surface, there are observable east-dipping thrust faults and east-north-east-striking cross faults distributed throughout the western limb of the Salin basin. Within the seismic section, the primary deep fore-thrust in the southwestern limb of the Chauk anticline originates within the PA Formation, as illustrated in **Figure 9**. As it progresses, it flattens out upon reaching the OKH and PY formations. These less competent strata of the OKH and PY formations induce disharmonic folding across and above them. The fold axis situated above the detachment level of the PY and OKH formations shifts further northeastward. The thickness of the growth strata in the PY and OKH formations increases due to the propagation of the deep-seated thrust.

Figure 10 presents the seismic profile cutting through the Letpando and Kyaukkwet anticlines located in the northern part of the Salin basin. According to Racey and Ridd[59], these 28 km long NW-SE Letpando and Kyaukkwet anticlines, which serve as traps, are compartmentalized by numerous cross faults. In the northeast limb of the Kyaukkwet anticlines, there is a deep-seated northeast-ward thrust. Notably, a deep hanging wall syncline in the northeast limb of the Kyaukkwet anticline introduces distinct fold geometry along this seismic profile. Consequently, above the crest of the deep anticline, a shallow low-angle fore-thrust pushes up into the growth strata, leading to the upward shift of the YA and SZT Formations within the Letpando anticline, as illustrated in **Figure 10**. The YA Formation is locally exposed along the structure's axis and serves as the primary seal, while sandstones in the underlying Eocene PO Formation function as the main reservoir, as noted by Racey and Ridd[59].

Seismic profiles reveal thrust faulting within the anticlines surrounding the Salin basin. This study specifically focuses on deep-seated structures within all anticlines and employs the interpretation of three seismic profiles (**Figures 8–10**). These anticlines were selected to conduct geological interpretations and detect any deep structures. The major thrust faults in these anticlines influence the geometry and kinematics of the folding. The Yenangyaung and Chauk thrust faults originate within the PA Formation, while the Letpando and Kyaukkwet anticlines have their roots in the TA Formation. The thickness of the OKH Formation increases from the fold hinge to the NE syncline, as evident in seismic profiles in **Figures 9–10**. Substantial thickness variations within the OKH Formation are attributed to ductile flow from the fold crest to the limbs. The disharmony of the fold axis above and below the OKH and PA formations is apparent, with these formations migrating toward the foreland. This disharmonic folding results from distinct mechanical behaviors of the formations during progressive deformation. In seismic section L-02 (**Figure 10**), low-angle shallow thrusts rooted within the PO and YA detachment zone indicate that deposition in front of these thrusts occurred concurrently with fault movements.

12. Conclusions

This study presents an initial interpretation encompassing seismic stratigraphy, structural analysis, hydrocarbon accumulation, and migration within the Salin basin. The investigation primarily focuses on a regional one-dimensional seismic survey, examining Formations spanning the Eocene to Pliocene epochs within the Salin basin. Within the study area, seven sequence boundaries and ten seismic sequences have been delineated. In ascending order, these seismic sequences are referred to as TL, TA, PO, YA, SZT, PA, OHK, PY, KK, and IRR. Correspondingly, the seismic boundaries include SBM, SBU, SB1, SB2, SB3, SB3, SB4, and SB6. The primary juxtaposition seal pertains to a fault that displaces a sealing lithology, often the top seal, into direct juxtaposition with the reservoir. The premise here is that the juxtaposed material remains impermeable over geological time. In contrast, secondary fault rock seals involve fault-zone material (fault rock) acting as a lateral seal. This is attributed to fault-induced grain-size reductions, the transportation of fine-grained material along the fault zone, and subsequent chemical processes leading to the formation of a continuous, low-permeability zone with a high capillary-entry-pressure threshold.

Gas chimneys, characterized as chaotic, disordered vertical disturbances observed in seismic section C-01 line at the central part of the Salin basin, play a significant role in the study. Identifying these gas chimneys provides crucial insights into the presence of hydrocarbons and enhances our understanding of the regional petroleum system. Additionally, it helps pinpoint potential over-pressured zones, thereby mitigating drilling risks. Once hydrocarbons mature within the source formation (comprising Eocene to Early Oligocene shale units), they follow predicted paths toward the reservoir formations (SZT, PA, and OHK).

Author contributions

Conceptualization, Methodology and Software: SNLA; Data curation: WM; Writing—original draft preparation: MTTA; Reviewing and Validation: AM; Writing—reviewing and Editing: KNNA. All authors have read and agreed to the published version of the manuscript.

Acknowledgments

The authors would like to thank Myanma Oil and Gas Enterprise (MOGE), Ministry of Electricity and Energy in Myanmar for supplying the data and samples for this study. We thank Kyi Khin and Prof. Khin Zaw for their suggestions for the earlier version of the manuscript, and the Editor-in-Chief and anonymous reviewers for our manuscript for their constructive comments to improve the manuscript.

Conflict of interest

The authors declare that they have no conflicts of interest related to the research presented in this work.

References

1. Kyi M. Biostratigraphy of the Central Burma Basin with special reference to the depositional conditions during Late Oligocene and Early Miocene times. *Union of Burma Journal of Science and Technology* 1970; 3: 75–90.
2. Aung SNL, He S, Han EM, et al. Organic geochemistry of crude oils from Oligocene reservoirs in the Salin Sub-basin, Myanmar: Insights into source, maturity, and depositional environment. *Journal of Asian Earth Sciences* 2021; 220: 104905. doi: 10.1016/j.jseaes.2021.104905
3. Htut T. Myanmar petroleum systems, including the offshore area. In: Barber AJ, Zaw K, Crow MJ (editors). *Myanmar: Geology, Resources, and Tectonics*. Geological Society, London, Memoirs; 2017. Volume 48. pp. 219–260. doi: 10.114 4/M48.11
4. Allan US. Model for hydrocarbon migration and entrapment within faulted structures. *American Association of Petroleum Geologists Bulletin* 1989; 73(7): 803–811. doi: 10.1306/44B4A271-170A-11D7-8645000102C1865D
5. Lindsay NG, Murphy FC, Walsh JJ, Watterson J. Outcrop studies of shale smears on fault surface. In: *The*

Geological Modelling of Hydrocarbon Reservoirs and Outcrop Analogues. Special Publication Int. Assoc. Sediment; 1993. pp. 113–123.
6. Fristad TA, Groth A, Yielding G, Freeman B. Quantitative fault seal prediction: A case study from Oseberg Syd. In: Møller-Pedersen P, Koestler AG (editors). *Hydrocarbon Seals: Importance for Exploration and Production*. Norwegian Petroleum Society Special Publication; 1997. Volume 7. pp. 107–124.
7. Fulljames JR, Zijerveld LJJ, Franssen RCMW. Fault seal processes: Systematic analysis of fault seals over geological and production time. In: Møller-Pedersen P, Koestler AG (editors). *Hydrocarbon Seals: Importance for Exploration and Production*. Norwegian Petroleum Society Special Publication; 1997. Volume 7. pp. 51–59.
8. Knipe RJ. Juxtaposition and seal diagrams to help analyze fault seals in hydrocarbon reservoirs. *American Association of Petroleum Geologists Bulletin* 1997; 81(2): 187–195. doi: 10.1306/522B42DF-1727-11D7-8645000102C1865D
9. Yielding G, Freeman B, Needham DT. Quantitative fault seal prediction. *American Association of Petroleum Geologists Bulletin* 1997; 81(6): 897–917. doi: 10.1306/522B498D-1727-11D7-8645000102C1865D
10. Bouvier JD, Kaars-Sijpesteijn CH, Kluesner DF, et al. Three-dimensional seismic interpretation and fault sealing investigations, Nun River Field, Nigeria. *American Association of Petroleum Geologists Bulletin* 1989; 73(11): 1397–1414. doi: 10.1306/44B4AA5A-170A-11D7-8645000102C1865D
11. Harding TP, Tuminas AC. Structural interpretation of hydrocarbon traps sealed by basement normal block faults at stable flank of foredeep basins and at rift basins. *American Association of Petroleum Geologists Bulletin* 1989; 73(7): 812–840. doi: 10.1306/44B4A276-170A-11D7-8645000102C1865D
12. Knipe RJ. Faulting processes and fault seal. In: Larsen RM, Brekke H, Larsen BT, Talleraas E (editors). *Structural and Tectonic Modelling and its application to Petroleum Geology*. Norwegian Petroleum Society Special Publications; 1992. pp. 325–342.
13. Gauthier BD, Lake SD. Probabilistic modeling of faults below the limit of seismic resolution in Pelican Field, North Sea, offshore United Kingdom. *American Association of Petroleum Geologists Bulletin* 1993; 77(5): 761–777. doi: 10.1306/BDFF8D4E-1718-11D7-8645000102C1865D
14. Berg RB, Avery AH. Sealing properties of tertiary growth faults, Texas Gulf coast. *American Association of Petroleum Geologists Bulletin* 1995; 79(3): 375–393. doi: 10.1306/8D2B1534-171E-11D7-8645000102C1865D
15. Barber CT. The natural gas resources of Burma. In: *Memoir Geological Survey India.* Geological Survey of India; 1935. Volume 66. pp. 1–172.
16. Pivnik DA, Nahm J, Tucker RS, et al. Polyphase deformation in a fore-arc/back-arc basin, Salin Subbasin, Myanmar (Burma). *American Association of Petroleum Geologists Bulletin* 1998; 82(10): 1837–1856. doi: 10.1306/1D9BD15F-172D-11D7-8645000102C1865D
17. Vail PR, Mitchum RM, Todd RG, et al. Seismic stratigraphy and global changes of sea level. In: Payton CE (editor). *Seismic Stratigraphy—Applications to Hydrocarbon Exploration*. AAPG Memoir; 1977. Volume 26. pp. 49–212.
18. Aung DW. *Oligocene-Miocene Sedimentary and Sequence Stratigraphy of the Northern Part of the Minbu Basin, Central Myanmar* [PhD thesis]. University of Yangon; 2006; Unpublished work.
19. Aung SNL, Han EM, Aung MTT. Thermal maturity assessment of Oligocene oil samples from central part Salin basin, Myanmar. In: Proceedings of the fourth Myanmar National Conference on Earth Sciences (MNCES); 28–29 December 2020; Taungoo, Myanmar.
20. Thein M, Maung M. The Eastern (Back-arc) Basin of Central Myanmar: Basement rocks, lithostratigraphic units, paleocurrents, provenance, and development history. In: Barber AJ, Zaw K, Crow MJ (editors). *Myanmar: Geology, Resources, and Tectonics*. Geological Society of London; 2017. Volume 48. pp. 169–183. doi: 10.114 4/M48.8
21. Htut T, Win T, Ko K, et al. *Geological Report of Thandwe-Gwa-Mawdin Pagoda Point Area (Rakhine Coastal Region North of Offshore Block A-6 Area)*. Myanma Oil and Gas Enterprise and MPRL E&P; 2008.
22. Khalifa M, Mills KJ. Seismic stratigraphic analysis and Structural development of an interpreted Upper Cambrian to Middle Ordovician sequence in the NW Blantyre Sub-basin, Darling Basin (western New South Wales, Australia). *Journal of Petroleum Geology* 2014; 37(2): 163–181. doi: 10.1111/jpg.12576
23. Rodriguez JLT, Lopez LAC. Seismic stratigraphic analysis on the off shore (Pelotas Basin). In: Proceedings of the 11th Bolivarian Symposium-Oil Exploration in the Subandean Basins (Spanish); 29 July–1 August 2012; Cartagena, Colombia. doi: 10.3997/2214-4609-pdb.330.105
24. Wornardt WW. Application of sequence stratigraphy to hydrocarbon exploration. In: Proceedings of the Offshore Technology Conference; 3–6 May 1993; Houston, USA. doi: 10.4043/7084-MS
25. Khin A. Hydrocarbon-producing formations of Salin, Irrawaddy, and Martaban Basins, Myanmar (Burma). In: Proceedings of the Society of Petroleum Engineers Asia-Pacific Conference; 4–7 November 1991; Perth, Australia. pp. 245–258.
26. Majid K, Shahid N, Munawar S, Muhammad H. Interpreting seismic profiles in terms of structure and stratigraphy with implications for hydrocarbons accumulation, an example from lower Indus basin Pakistan. *Journal of Geology and Geophysics* 2016; 5(5): 257. doi: 10.4172/2381-8719.1000257
27. Catuneanu O. *Principles of Sequence Stratigraphy*. Elsevier; 2006. 375p.
28. Sangree JB, Widmer JM. Seismic stratigraphy and global changes of sea level, part 9: Seismic interpretation of

clastic depositional facies. In: Payton CE (editor). *Seismic Stratigraphy–Applications to Hydrocarbon Exploration.* American Association of Petroleum Geologists Memoir; 1977. Volume 26. pp. 165–184.
29. Hackbarth CJ, Shew R. Morphology and stratigraphy of a mid-Pleistocene turbidite leveed channel from the seismic, core, and log data, northeastern Gulf of Mexico. In: Weimer P, Bouma AH, Perkins BF (editors). *Submarine Fans and Turbidite Systems*. SEPM Society for Sedimentary Geology; 1994. pp. 127–133. doi: 10.5724/gcs.94.15.0137
30. Htay HH. *Stratigraphy and Sedimentology of The Seikpyu-Chauk Area, Magway Region* [PhD thesis]. University of Mandalay; 2012; Unpublished work.
31. Beard DC, Weyl PK. Influence of texture on porosity and permeability of unconsolidated sand. *American Association of Petroleum Geologists Bulletin* 1973; 57(2): 349–369. doi: 10.1306/819A4272-16C5-11D7-8645000102C1865D
32. Wandrey CJ. *Eocene to Miocene Composite Total Petroleum System, Irrawaddy-Andaman, and North Burma Geologic Provinces, Myanmar*. In: Wandrey CJ (editor). U.S. Geological Survey Bulletin 2208-E; 2006. p. 26.
33. Hamad M, El-Gammal RM, Lwin SM, Aung MM. Provenance, tectonic setting & geochemical maturity of the early Miocene Pyawbwe formation, Sakangyi–Thayet area, Magway region, Myanmar. *Geopersia* 2018; 8(1): 1–13. doi: 10.22059/geope. 2017.230212.648314
34. Ko MM. *Sequence and Event Stratigraphy of the Oligocene Limestones Exposed at Thebu-Yegyanzin Area, Thayet and Mindon townships, Magway Region* [PhD thesis]. University of Mandalay; 2012; Unpublished work.
35. Sturt CJ, Curial JA, Filewicz MV, et al. *Sequence Stratigrapgy Framework, biostratigraphy, Organic Geochemistry, Basin Evolution and Stratigraphic Trapping, Potential of block 'F' area, Central Myanmar Basin*. Unocal Myanmar LTD; 1992.
36. Aung DA. Sedimentology of Oligocene clastic strata in the western part of the Minbu Basin, Myanmar. In: Proceedings of the GeoMyanmar 2012, First International Conference on Myanmar Geology; 1–2 March 2012; Yangon, Myanmar. p. 28.
37. Yamaguchi T, Suzuki H, Soe AN, et al. A new late Eocene Bicornucythere species (Ostracoda, Crustacea) from Myanmar, and its significance for the evolutionary history of the genus. *Zootaxa* 2015; 3919(2): 306–326. doi: 10.11646/zootaxa.3919.2.4
38. Aung AK. Revision of the stratigraphy and age of the primate-bearing Pondaung Formation. In: Proceedings of the Pondaung Fossils Expedition Team; 1999; Yangon, Myanmar. pp. 131–178.
39. Aung AK. The primate-bearing Pondaung Formation in the upland area, northwest of central Myanmar. In: Ross C, Kay RF (editors). *Anthropoid Origins: New Visions*. Kluwer Academic/Plenum Publishers; 2004. pp. 205–217.
40. Soe AN, Tun ST, Aung AK, et al. Sedimentary facies of the late middle Eocene Pondaung Formation (central Myanmar) and the palaeoenvironments of its anthropoid primates. *Comptes Rendus Palevol* 2002; 1(3): 153–160. doi: 10.1016/S1631-0683(02)00020-9
41. Lwin SM, Aung MM, Oo NP. Paleoenvironmental analysis of benthic foraminifera and radiolarians in middle Eocene Tabyin Formation, Mindon-Taing Da area, Magway region, Myanmar. In: Proceedings of the Third AAPG/EAGE/MGS Oil and Gas Conference; 22–24 February 2017; Yangon, Myanmar.
42. Corona FV, Davis JS, Hippler SJ, Vrolijk PJ. Multi-fault analysis scorecard: Testing the stochastic approach in fault seal prediction. In: Jolley SJ, Fisher QJ, Ainsworth RB, et al. (editors). *Reservoir Compartmentalization*. Geological Society, London, Special Publications; 2010. Volume 347. pp. 317–332. doi: 10.1144/SP347.18
43. Bretan P. Trap analysis: An automated approach for deriving column height predictions in fault-bounded traps. *Petroleum Geoscience* 2017; 23(1): 56–69. doi: 10.1144/ 10.44 petgeo 2016-022
44. Murray TA, Power WL, Johnson AJ, et al. Validation and analysis procedures for juxtaposition and membrane fault seals in oil and gas exploration. In: Ogilvie SR, Dee SJ, Wilson RW, Bailey WR (editors). *Integrated Fault Seal Analysis*. Geological Society, London, Special Publications; 2020. Volume 496. pp. 145–161. doi: 10.1144/SP496-2018-171
45. Klarner S, Kirnos D, Klarner O, et al. Fault seal analysis from seismic and well data. In: Proceedings of the Far East Hydrocarbons 2016; 4–6 October 2016; Yuzhno-Sakhalinsk, Russia. pp. 1–5. doi: 10.3997/2214-4609.201602321
46. Tao Z. *Crestal Fault Reactivation on Rising Salt Diapirs: An Integrated Analysis from Large to Small Scales of Observation* [PhD Thesis]. Cardiff University; 2018.
47. Singh D, Kumar PC, Sain K. Interpretation of gas chimney from seismic data using artificial neural network: A study from Maari 3D prospect in the Taranaki Basin, New Zealand. *Journal of Natural Gas Science and Engineering* 2016; 36: 339–357. doi: 10.1016/j.jngse.2016.10.039
48. Heggland R. Definition of geohazards in exploration 3-D seismic data using attributes and neural-network analysis. *American Association of Petroleum Geologists Bulletin* 2004; 88(6): 857–868. doi: 10.1306/02042004
49. Hustoft S, Mienert J, Bunz S, Nouze H. High-resolution 3D-seismic data indicate focused fluid migration pathways above polygonal fault systems of the mid-Norwegian margin. *Marine Geology* 2007; 245(1–4): 89–106. doi: 10.1016/j.margeo.2007.07.004
50. Hustoft S, Bunz S, Mienert J. Three-dimensional seismic analysis of the morphology and spatial distribution of chimneys beneath the Nyegga pockmark field, offshore mid-Norway. *Basin Research* 2010; 22(4): 465–480. doi: 10.1111/j.1365-2117.2010.00486.x

51. Petersen CJ, Bunz S, Hustoft S, et al. High-resolution P-Cable 3D seismic imaging of gas chimney structures in gas hydrated sediments of an Arctic sediment drift. *Marine and Petroleum Geology* 2010; 27(9): 1981–1994. doi: 10.1016/j.marpetgeo.2010.06.006
52. Aminzadeh F, Connolly D, De Groot P. Interpretation of gas chimney volumes. In: *SEG Technical Program Expanded Abstracts 2002*, Proceedings of the SEG 72nd Exposition and Annual Meeting; 6–11 October 2002; Salt Lake City, USA. Society of Exploration Geophysicists; 2002.
53. Ho S, Carruthers D, Imbert P. Insights into the permeability of polygonal faults from their intersection geometries with Linear Chimneys: A case study from the Lower Congo Basin. *Carnets Geol* 2016; 16(2): 17–26.
54. Tankard AJ, Balkwill HR, Mehra A, Din A. Tertiary wrench tectonics and sedimentation in the central basin of Myanmar. Available online: https://archives.datapages.com/data/meta/cspg_sp/data/CSPG-SP-016/016001/pdfs/62_firstpage.pdf (accessed on 20 September 2023).
55. Khin K, Moe A, Aung KP, Zaw T. Structural and tectonic evolution between Indo-Myanmar ranges and central Myanmar Basin: Insights from the Kabaw Fault. *Geosystems and Geoenvironment* 2023; 2(2): 100176. doi: 10.1016/j.geogeo.2022.100176
56. Fischer MP, Woodward NB, Mitchell MM. The kinematics of break-thrust folds. *Journal of Structural Geology* 1992; 14(4): 451–460. doi: 10.1016/0191-8141(92)90105-6
57. Ghosh SK. *Structural Geology-Fundamentals and Modern Developments*. Pergamon Press; 1993. 598p.
58. Khin K, Moe A, Aung KP. Tectono-structural framework of the Indo-Myanmar Ranges: Implications for the structural development on the geology of the Rakhine Coastal Region, Myanmar. *Geosystems and Geoenvironment* 2022; 1(3): 100079. doi: 10.1016/j.geogeo.2022.100079
59. Racey A, Ridd MF. *Petroleum Geology of Myanmar*. The Geological Society; 2015. 45p.